Performance evaluation of gravity-controlled rocking braced frames for low-rise steel buildings

Paul Mottier[1], Lydell Wiebe[2], Taylor Steele[3], Robert Tremblay[4], Colin Rogers[5]

[1] Ph.D. Student, Dept. of Civil, Geological and Mining Engineering, Polytechnique Montreal, Montreal, QC, Canada
[2] Associate Professor, Dept of Civil Engineering, McMaster University, Hamilton, ON, Canada.
[3] Ph.D. Student, Dept of Civil Engineering, McMaster University, Hamilton, ON, Canada.
[4] Professor, Dept. of Civil, Geological and Mining Engineering, Polytechnique Montreal, Montreal, QC, Canada
[5] Associate Professor, Dept. of Civil Engineering and Applied Mechanics, McGill University, Montreal, QC, Canada

ABSTRACT

This article presents a seismic performance evaluation of gravity-controlled rocking braced frame buildings. The prototype structures are three- and six-storey buildings located in a region of high seismicity in the United States. Chevron bracing is used in the frames, and friction-based energy dissipation is added as part of the design. The OpenSees software is used to develop models that are validated against past experimental studies and the performance is assessed using nonlinear dynamic analyses with representative ground motion record sets for the building location. The performance of the buildings in terms of drifts and force demands is compared with previous results for buildings with controlled rocking braced frames that rely on post-tensioning tendons. The results of the study show that the gravity-controlled rocking braced frame buildings require more frames to resist the same seismic loads, but this has the benefit of leading to reduced peak interstorey drifts. The force demands induced by impact in the gravity-controlled rocking braced frames are always less than the squash load of the columns and are more significant for the three-storey building than for the six-storey building. Overall, the results suggest that both types of controlled rocking braced frame show promise as effective ways to resist seismic loads without structural damage.

Keywords: self-centring systems; controlled rocking steel braced frames; impact loading; gravity loads; nonlinear time history analysis.

INTRODUCTION

While current codes prescribe numerous methods to efficiently ensure that the life of the occupants is preserved during major earthquakes, recent examples have shown that economic losses due to earthquakes could be severe and thus should be given more consideration when designing new buildings [1]. For several decades, rocking systems have been increasingly studied and are considered as a very promising way to design resilient buildings against earthquakes [2]. Their ability to withstand major earthquakes without residual drifts has been proven through several experimental studies [3-5] and real-life examples [6-7]. Among these rocking structures, steel controlled rocking braced frames (CRBFs) have shown their efficiency to reduce demands in the braced frame members during earthquakes, relative to an equivalent fixed-base building. These structures often rely on vertical post-tensioning to self-centre the building and energy dissipative (ED) devices to help control drifts [8]. Several design methods have been developed for CRBFs [4, 8-10]. Recent studies produced regression equations to capture the expected drifts of such structures [11] and gave guidelines to capacity-design the frame members considering the additional demands due to higher modes effects while rocking [12]. However, these methods and guidelines focused on controlled rocking frames that rely on post-tensioning (PT) tendons to re-centre the building, referred to as PT-CRBFs. In this configuration, the floor system is decoupled from the rocking frame in the vertical direction. Conversely, a controlled rocking braced frame may also be designed using gravity loads to re-centre, referred to as gravity-controlled rocking braced frames (G-CRBFs). In this configuration, the floor system must uplift along with the rocking frame. Therefore, impacts between the column and its foundation when the frame returns to its original position induce vertical inertia forces that can increase the demands in the frame members. This solution has been numerically and experimentally studied recently, giving promising results [13-14].

This paper presents an assessment of the seismic performance of G-CRBFs and aims at comparing the responses of PT-CRBFs and G-CRBFs. To do so, two buildings from a study performed previously [12] are redesigned to be G-CRBFs buildings. A model of each building is subjected to 44 ground motions records scaled to the maximum considered earthquake (MCE) level. The response is compared to the design predictions in terms of drifts and force demands for the G-CRBF building. Finally, the performance of the PT-CRBF and the G-CRBF buildings are compared.

DESIGN METHODOLOGY

Two different heights of building were designed for a site of high seismicity in the Western United States. The seismic design data were taken as $S_S = 1.5g$, $S_1 = 0.6g$, $F_a = 1.0$ and $F_v = 1.5$, assuming the site to be class D according to ASCE 7-16 [15]. Each storey was assumed to have the same height of 4.57 m. The buildings were considered to be 6 bays wide and 4 bays long, each bay being 9.15 m wide. The seismic weights were equal to 6430 kN at the roof level and 9430 kN at the floor levels, assuming dead load values of 3.2 kPa at the roof level and 4.1 kPa at the floors.

The base rocking joints of the studied G-CRBFs buildings were designed using the equivalent static procedure described by Steele and Wiebe [12]. The response modification factor was chosen to be equal to the maximum value permitted by ASCE 7-16 [15], $R = 8$, which was also the value chosen in the earlier study [12]. The ED value activation force was selected so that the rocking moment given by Eq. (1) $M_{b,rock}$, was higher than the minimum overturning moment $M_{b,min}$:

$$M_{b,rock} = M_{ED} + M_W \geq M_{b,min} \tag{1}$$

In Eq. (1), M_{ED} is the resisting moment to overturning given by the ED device and M_W is the moment conferred by the gravity loads carried by the frame. The ED value was also required to be less than or equal to the dead load on each column in order to guarantee that the frame would self-centre after the earthquake. The ED device was chosen to be a friction device, as such a system is easily installed and replaced. Once the activation force of the ED device was selected, the number of frames and their locations were chosen. As the G-CRBFs buildings cannot rely on PT tendons to self-centre, different design choices were required compared to the PT-CRBFs. Considering that the geometry of the building was assumed to be imposed (bay width constant and equal to 9.15 m), the choice of the ED value fully defined the rocking moment of each G-CRBF. This resulted in a reduced effective value of $R_{eff}=R/\Omega$, where Ω represents the overstrength factor of the frame.

Next, the contribution from higher modes was computed using the equations for the static method defined previously [12]. No amplification was applied to account for impact while rocking. The higher mode forces were computed using the MCE-level scaled spectrum, as presented in Figure 1a. All the frame members were capacity designed based on the combined forces applied to each member and according to the requirements prescribed in AISC 360-16 [16] for axial compression only (braces and columns) and for combined axial compression and bending moment (beams). A k factor of 0.9 was used for all members.

At the end of the design process, the drifts were checked to be less than a 2.5% limit, as has been suggested previously [5]. Though ASCE 7-16 [15] prescribes the use of C_d in the calculation of the displacements, the lateral displacements considering nonlinear effects (Δ_x) were computed according to Eq. (2) [11], to consider that the equal displacement assumption is often not conservative for rocking structures. In that equation, Δ_{xe} is the lateral deflection determined from elastic analysis, I_e is the importance factor assigned to the building and C_R is the displacement ratio used to consider the drifts for a rocking building and was chosen to be calculated based on the initial stiffness proportional damping.

$$\Delta_x = \Delta_{xe} \frac{R_{eff}}{I_e} C_R \tag{2}$$
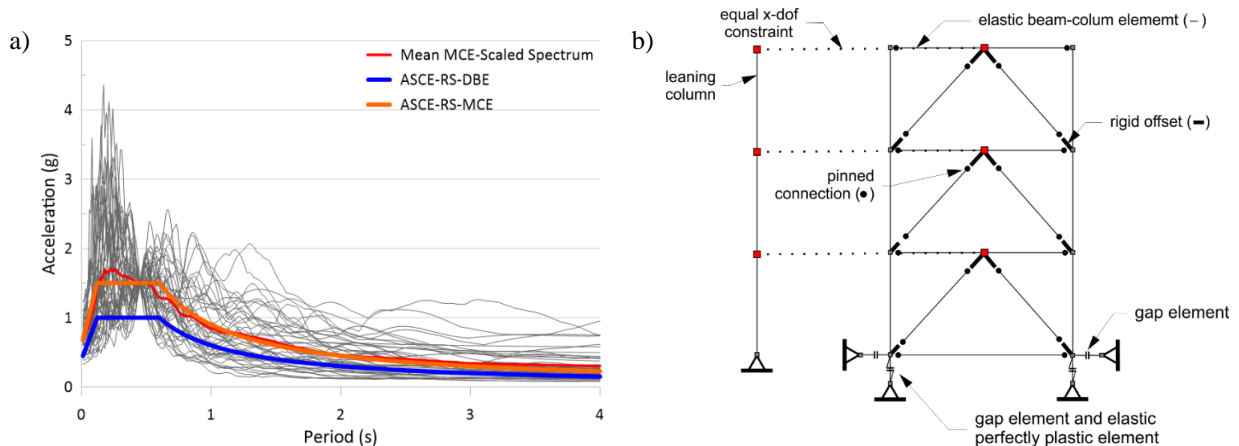

Figure 1 – Data used for the study: (a) MCE-scaled response spectrum. (b) illustration of the numerical model used.

The PT-CRBF designs that were studied previously [12] are given in the first line of Tables 1 and 2 for three and six storeys, respectively. In Tables 1 and 2, N_f is the number of frames per building in each direction; β represents the ED ratio, defined as the ratio of $2M_{ED}$ to $M_{b,rock}$; η is the post-tensioning prestress ratio defined as the ratio of initial (PT_0) to ultimate (PT_u) post-tensioning force, when applicable; $M_{b,max}$ is the maximum expected overturning moment at the base; Ω is the system

overstrength; $T_{1,est}$ is the code estimate of the first-mode period; and T_1 and T_2 are the first-mode and second-mode periods from the modal analysis in OpenSees. An alternative G-CRBF is summarized in the second line of each of Tables 1 and 2. For all designs the frames were assumed to be located on the edge of the building. Tables 1 and 2 show that due to the absence of post-tensioning tendons in the G-CRBF designs, N_f had to be doubled to match the targeted value of *R*.

Table 1 Base rocking joint parameters of the designed three-storey buildings

Design	N_f	R	R_{eff}	$M_{b,min}$ (kNm)	β	ED (kN)	η	PT_0 (kN)	PT_u (kN)	M_W (kNm)	$M_{b, rock}$ (kNm)	$M_{b, max}$ (kNm)	Ω	$T_{1,est}$ (s)	T_1 (s)	T_2 (s)
3S-R8	2	8	7.9	16690	0.90	910	0.52	2040	3910	553	16710	24390	1.46	0.487	0.547	0.188
G-3S-R8	4	8	5.9	8004	0.92	550	N/A	N/A	N/A	5897	10930	10930	1.37	0.487	0.418	0.159

Table 2 Base rocking joint parameters of the designed six-storey buildings

Design	N_f	R	R_{eff}	$M_{b,min}$ (kNm)	β	ED (kN)	η	PT_0 (kN)	PT_u (kN)	M_W (kNm)	$M_{b, rock}$ (kNm)	$M_{b, max}$ (kNm)	Ω	$T_{1,est}$ (s)	T_1 (s)	T_2 (s)
6S-R8	2	8	7.9	50790	0.89	2770	0.52	3120	5990	1554	51440	74620	1.47	0.819	1.058	0.335
G-6S-R8	4	8	7.9	24050	0.94	1250	N/A	N/A	N/A	12905	24342	24342	1.01	0.819	0.893	0.282

MODELLING

The frame was modelled in two dimensions using OpenSees [17], as shown in Figure 1b. All frame members were modelled using elastic beam-column elements with a corotational geometric transformation to capture the full elastic force demand induced by the higher mode responses. Gusset plates were modelled as elastic rigid offsets. Braces and beams were assumed to be pinned at their extremities. Uplift was modelled using gap elements with a compression stiffness equal to the axial stiffness of the vertical column near the base. The frictional ED devices were included as elastic perfectly plastic elements with a yield force equal to the activation force. Dead loads, including the self-weight of the selected section of the frame, were applied as lumped masses at each column node and as linearly distributed masses on the beams, with a constant vertical acceleration of 1.0g to develop the associated forces in the frame. The frame mass was defined as a consistent mass matrix option for columns and braces.

P-Delta effects were captured using a pinned-base leaning column with elastic beam-column elements having the total area of the gravity columns within the tributary area for seismic mass but with a negligible bending moment of inertia. Horizontal masses representing the tributary seismic weight of the whole building were applied on the leaning column nodes and were constrained to have the same lateral displacement as the middle frame nodes to simulate the transfer of the seismic forces from the diaphragm.

Tangent stiffness-proportional Rayleigh damping was applied assuming a damping ratio of 5% in modes one and two using the fixed-base periods of the frame. No damping was assigned to the rocking elements (gap or ED elements).

RESPONSE TO EXAMPLE GROUND MOTION

Each numerical model was subjected to the 44 ground motions given in the FEMA P695 ground motions set [18] scaled to the MCE level. Figure 2 presents the seismic response of the G-CRBF three-storey building under a representative ground motion showing that the earthquake induces successive uplift cycles in the frame. Vertical lines represent the instant of impact of the G-CRBF columns. The response of the equivalent PT-CRBF building to the same ground motion is plotted on the same figure. The behaviour of the two buildings is very similar, both in terms of dynamic base shear and in terms of drifts. The dynamic base shear developed in the PT-CRBF building appears to be composed of a higher frequency content in comparison with the G-CRBF building, which may be because the PT tendons are still acting on the frame during the earthquake, even as the frame rocks.

Figures 3 and 4 show the compression demands in the columns and the braces. The expected design load, based on the methodology presented earlier, is shown by a dashed blue line. The demands in the frame members may be divided into two phases. First, immediately after each impact, high peaks of compression demands are induced in the frame members. These are significantly higher than the demands during the rocking phase, because of inertia forces due to the vertical movement of the floors and gravity framing. For the selected earthquake, the force demands during the impacts are higher than the design values

but not as large as the compressive squash load, defined as $P_y=AF_y$ where A is the net section of the selected member and F_y the yield stress of the material. The magnitude of the demand is not accurately captured by the design method, especially for the roof level column, with a ratio of demands to design forces that is as high as 3. At the other levels, the member forces are slightly higher than the design loads. This phase generally lasts less than 0.3 s. Though the design predictions are exceeded, this does not necessarily imply that the integrity of the frame is damaged. This is because the compressive loads due to impacts have a frequency up to three times the eigen frequency of the members; as such, a column member is not fully compressed along its whole length at any given time. Moreover, the dynamic resistance of a member in compression is higher than its static compression capacity [19]. Based on these considerations, the squash load has been used as a comparison to determine a threshold of compression demands after impact beyond which the structural integrity of the members is more likely to be affected. Second, after the impact phase is over, the force demands in the members are well captured by the design method, until the next impact of the column.
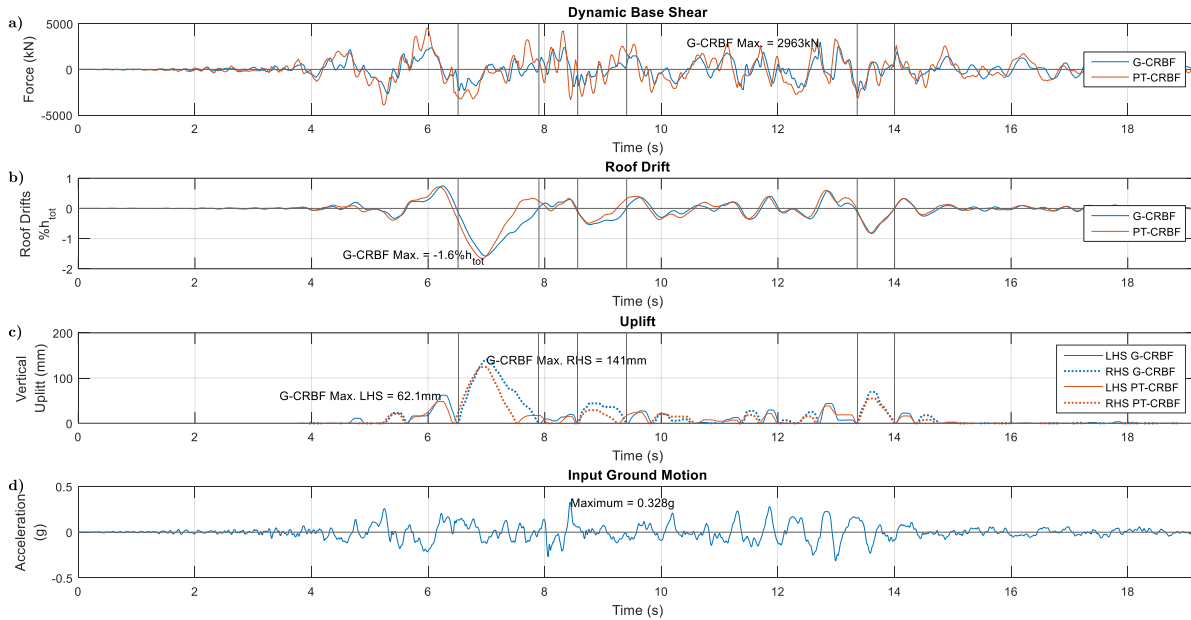

Figure 2 - Main response parameters of the three-storey G-CRBF to ground motion RSN1787Hector HEC090: a) Base shear; b) Roof drift; c) Vertical uplift; d) Ground motion.

RESPONSE TO ALL GROUND MOTIONS

Peak Interstorey Drifts

Table 3 lists the average maximum roof drifts of the studied buildings. As explained earlier, the design predictions are computed using Eq. (2) given by Zhang et al. [11]. The use of C_R predicts the drifts to within 20% accuracy for the designs 3S-R8, 6S-R8 and G-6S-R8, but not for G-3S-R8 for which the prediction was unconservative (ratio of analysis mean to design prediction higher than 1.0) by a factor of 1.54. Overall, the drifts are larger for the PT-CRBF buildings, likely because the PT-CRBF buildings have half the number of frames compared to the G-CRBF building, and thus are more flexible.

Table 3 Maximum Roof Drifts results of the PT- and G-CRBF building

Design	R_{eff}	C_R	Δ_{xe}	Drifts (% h_{tot})		
				Design Prediction	Analysis Mean	Ratio AM/DP
3S-R8	7.9	2.27	0.121	2.16	2.54	1.18
G-3S-R8	5.9	2.56	0.082	1.23	1.90	1.54
6S-R8	7.9	1.48	0.193	2.25	1.85	0.82
G-6S-R8	7.9	1.60	0.129	1.63	1.70	1.05

Peak Force Demands in G-CRBF

The peak member compression demands in the G-CRBFs from all ground motions are shown in Figure 5. These results confirm that the force demands during impact govern the peak compression demands in the frame members for all the ground motions. For example, for the three-storey building, the mean force demand in the column is higher than the design predictions by a

factor of 1.1 in the first storey up to a factor of 3.1 in the top storey. The force demands during impact significantly increase the mean and the median of the force demands in the braces as well; the means at the second storey and at the roof are 1.7 times and 1.2 times the design predictions respectively. The peak axial compressions in the beam are less affected by the force demands during impact, as the vertical inertia forces tend to increase the moment in the beam but not the axial compression directly. The mean of the force demands in the beam is equal to 0.85 times the design prediction at the first and third storeys, and 1.3 times the design expectation at the second storey.

For the six-storey building, the mean of the force demands in the columns is higher than the design predictions at all storeys but the first storey, with the ratio of mean of force demands to design predictions varying from 1.6 at the roof level to 0.9 at the first storey level. From the second to the fifth storey, the demands are higher than the design predictions by a factor of approximately 1.05. However, for the same storeys, the median is significantly less than the design predictions (by a factor of approximately 0.85). In the braces and the beams, the mean of the demands varies from 0.95 to 1.1 times the design predictions, suggesting that the forces induced during impact are not as significant as in the three-storey building. For all members in both frame heights, both the mean and the median value are less than the compressive squash load for every considered ground motion.
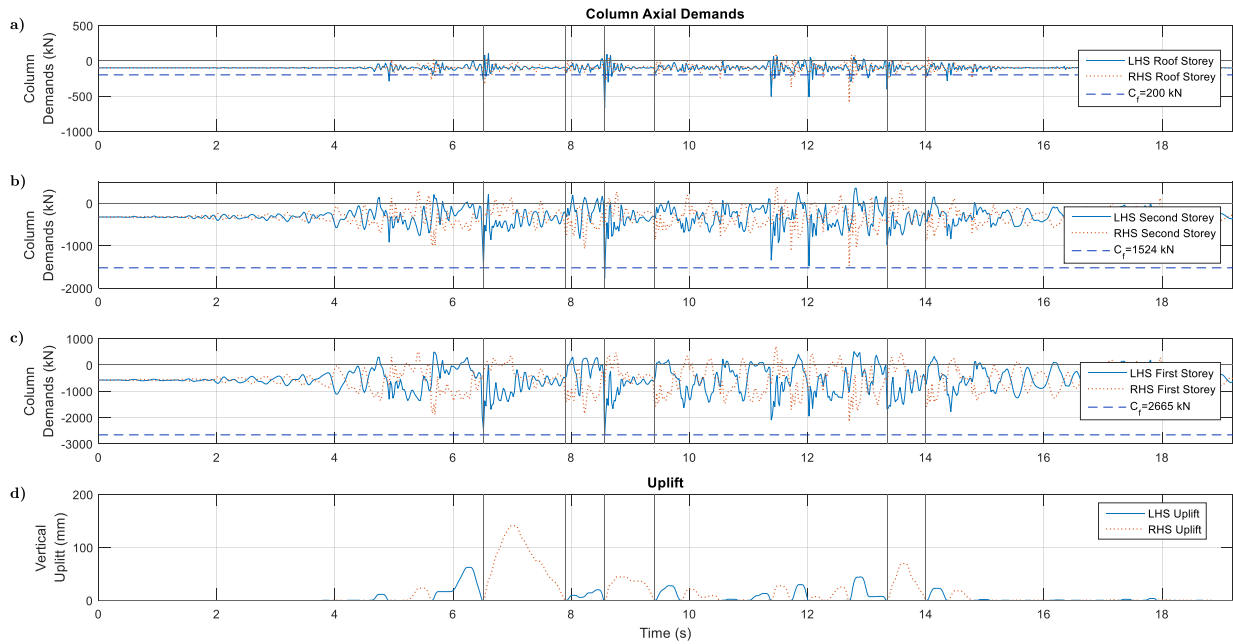

Figure 3 Peak axial compression demands on columns under a seismic excitation for three-storey G-CRBF building: a) Roof level; b) Second Storey; c) First Storey; d) Vertical uplift.

Comparison of Peak Forces in G-CRBF and PT-CRBF

Figure 6 shows the peak demands in the framing members for the three- and six-storey PT-CRBF buildings. As can be seen, the design method captures the demands in the frame members slightly more accurately when post-tensioning is used. Contrary to the G-CRBF building, the design predictions of the PT-CRBF building are slightly higher than peak demands for the braces and for the columns. This is because the PT-CRBF does not have significant inertia effects caused by impacts because the uplifting mass is relatively small.

Table 4 lists the ratio of the force demands in the G-CRBF buildings to the force demands in the corresponding PT-CRBF buildings. Although the magnitude of the mean demands appears to be less in the G-CRBF, this is because the number of frames with the G-CRBF design was divided by two in comparison with the PT-CRBF design. For the three-storey building, PT tendons were located in the middle of the frame: this explains that the demand on the roof level columns was higher in the G-CRBF building. In contrast, in the six-storey buildings, PT tendons were located on the column of the frame, which explains why the demands on the columns were higher in the PT-CRBF building for that case.

As shown in Table 4, for the three-storey building, the ratio of the force demands in each member is higher than 0.5, except in the brace at roof level. This shows that the force demands are increased in the G-CRBF building in comparison with the PT-CRBF building, suggesting that the force demands induced during impact have a significant relative influence on low-rise buildings. For the six-storey building, the ratio of the mean force demands in the G-CRBF building to the PT-CRBF building

is slightly less than 0.5 in all members except the roof beam. This suggests that for the considered mid-rise building, the forces induced during impact were not significant relative to those that developed without impact.
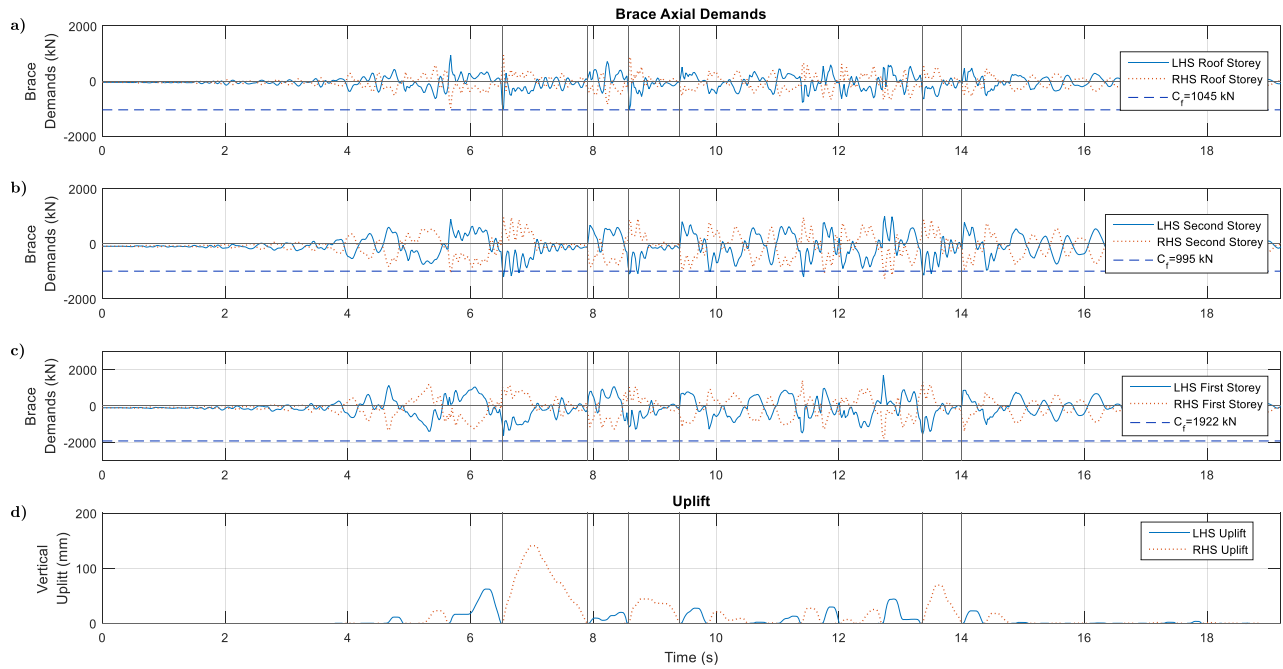

Figure 4 - Peak axial compression demands on braces under a seismic excitation for three-storey G-CRBF building: a) Roof level; b) Second Storey; c) First Storey; d) Vertical uplift.
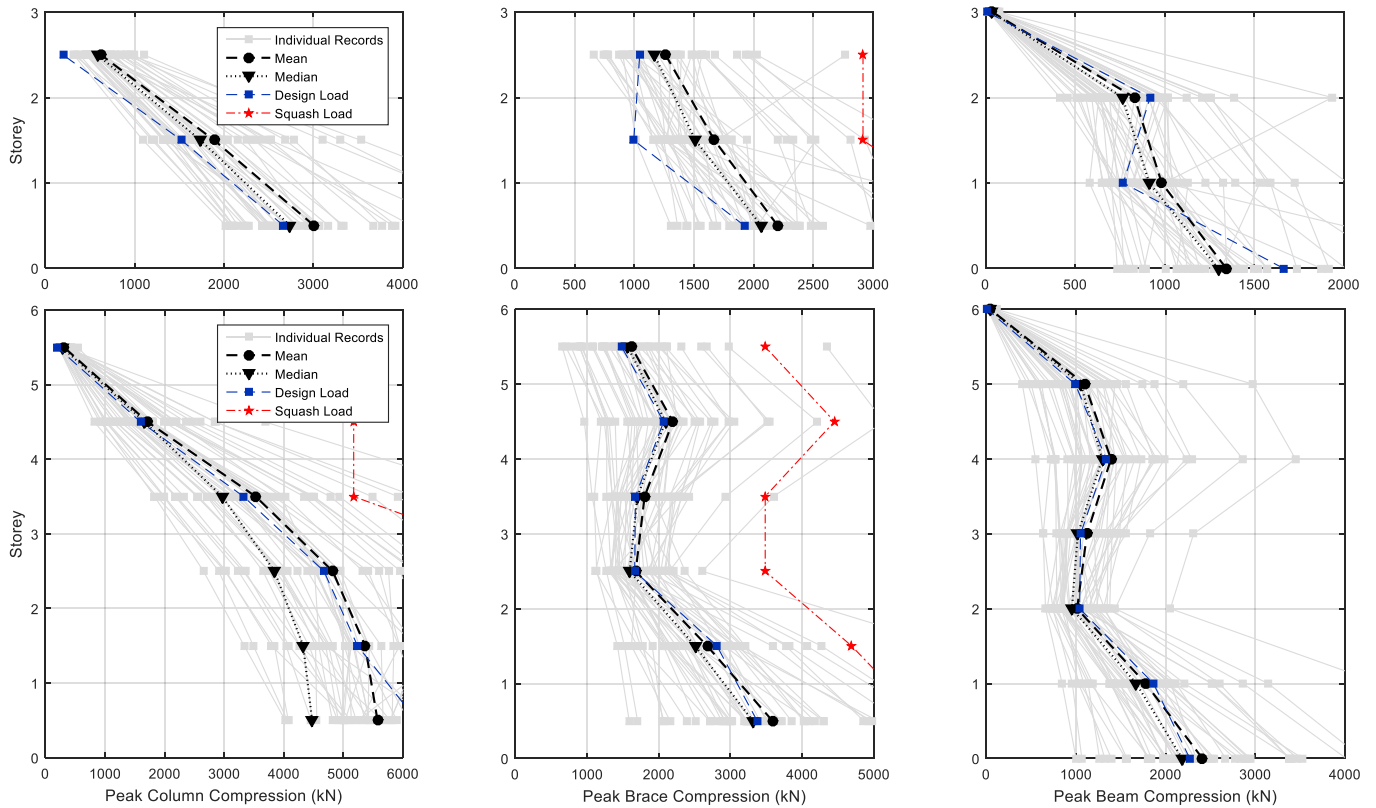

Figure 5 - Peak member compressions for the three- and six-storey G-CRBF buildings.
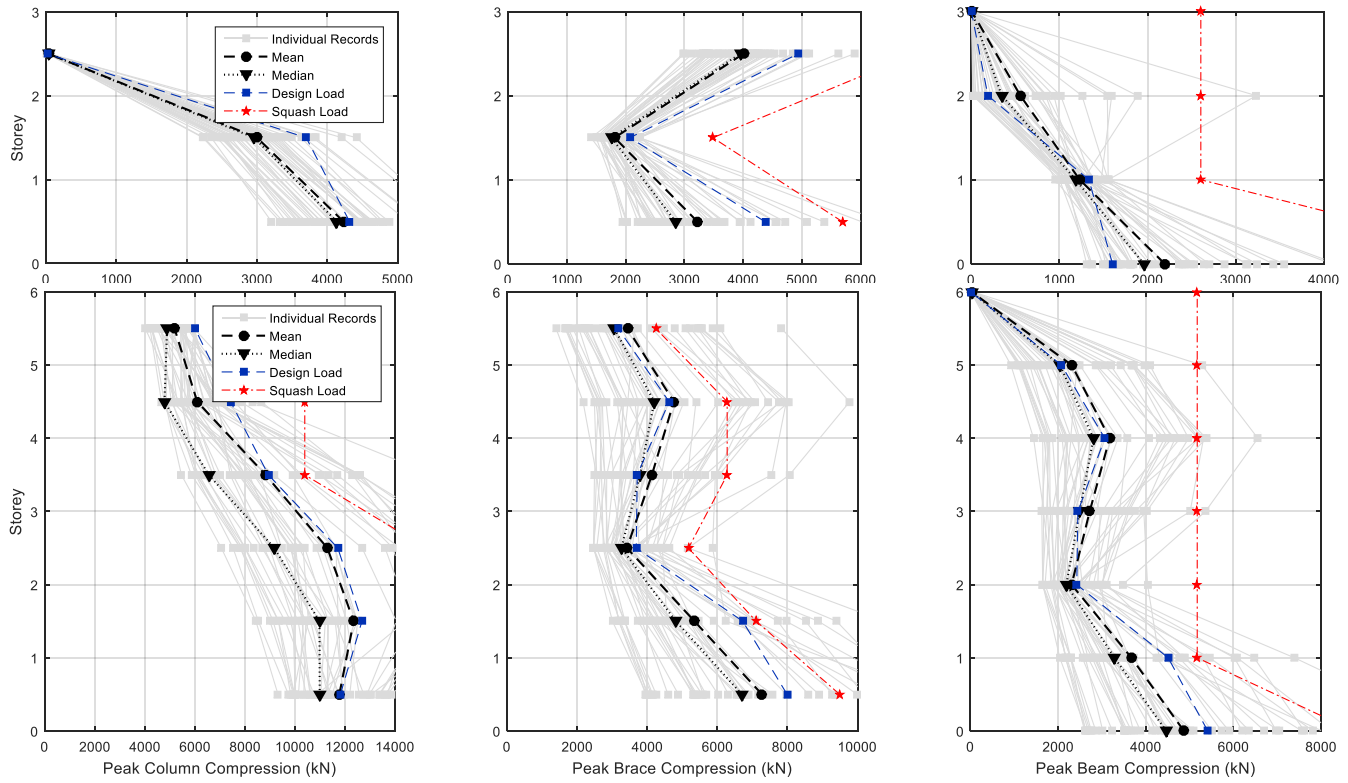
Figure 6 - Peak member compression for the three- and six-storey PT-CRBF buildings.

Table 4 Ratio of the mean force demands in one G-CRBF frame to those in one PT-CRBF frame

Storey	Three-Storey Building			Six-Storey Building		
	Column	**Brace**	**Beam**	**Column**	**Brace**	**Beam**
0	-	-	0.61	-	-	0.49
1	0.71	0.68	0.80	0.47	0.49	0.48
2	0.63	0.92	1.49	0.44	0.50	0.44
3	16.5	0.31	5.09	0.43	0.49	0.41
4	-	-	-	0.40	0.44	0.44
5	-	-	-	0.28	0.46	0.47
6	-	-	-	0.06	0.47	1.51

Note: Each building has 4 G-CRBF frames in each direction and 2 PT-CRBF frames in each direction.

CONCLUSION

A building with gravity-controlled rocking braced frames was designed by adapting a methodology previously proposed for post-tensioned PT-CRBFs. This study aimed at assessing the seismic response of G-CRBFs and comparing it with the response of corresponding PT-CRBFs. Nonlinear response history analyses were performed in OpenSees for representative ground motions. The study showed that the average drifts were reduced in the G-CRBF building in comparison with the PT-CRBF building. However, this came at the expense of having twice the number of rocking frames, as the rocking load of each was reduced by having no post-tensioning. Results showed that the force demands in three-storey G-CRBF braces and columns are governed by the effects of impact, due to the vertical movement of the gravity framing system. For that reason, the magnitude of force demands in the G-CRBF building is higher than in the PT-CRBF building. The design method that was developed for PT-CRBFs was not intended to capture the compression demands imposed by such impacts. However, shortly after the impact the compression demands in all the members are quite well captured by the prescribed design method. Further research is needed to assess the effect of these impacts and to determine whether they are likely to endanger the structural integrity of the

frame, given the short duration during which the high compression demands happen. The consequences of column impacts were less pronounced for the six-storey G-CRBF buildings, and the magnitude of the demands in the six-storey building frame members was similar in both of the two studied design approaches, after accounting for the difference in the number of frames due to the difference of self-centring mechanisms. Overall, the results show that the G-CRBF is a promising system for new buildings.

ACKNOWLEDGMENTS

REFERENCES

[1] Canterbury Earthquakes Royal Commission. (2012). *Summary and Recommendations in Volumes 1-3, Seismicity, Soils and the Seismic Design of Buildings*. Final report: Volume 1. *Wellington, New Zealand*.

[2] Housner, G.W. (1963). "The Behaviour of Inverted Pendulum Structures During Earthquakes". *Bulletin of the Seismological Society of America*, 53(2): 403-417.

[3] Midorikawa, M., Azuhata, T., Ishihara, T., and Wada, A., (2006). "Shaking table tests on seismic response of steel braced frames with column uplift", *Earthquake Engineering and Structural Dynamics*, *35*(14),1767-1785.

[4] Ma, X., Deierlein, G., Eatherton, M., Krawinkler, H., Hajjar, J., Takeuchi, T., Kasai, K., Midorikawa, M., and Hikino, T. (2010) "Large-scale shaking table test of steel braced frame with controlled rocking and energy dissipating fuses". In *Proceedings of the 9th US and 10th Canadian Conference on Earthquake Engineering*, Toronto, ON.

[5] Wiebe, L., Christopoulos, C., Tremblay, R., and Leclerc, M., (2013). "Mechanisms to limit higher mode effects in a controlled rocking steel frame. 1: Concept, modelling, and low-amplitude shake table testing", *Earthquake Engineering and Structural Dynamics*, 42(7): 1053-1068.

[6] Latham, D.A., Reay, A.M. and Pampanin, S., (2013). "Kilmore Street Medical Centre: application of a post-tensioned steel rocking system". In *Proceedings Steel Innovations Conference 2013*, Christchurch, New Zealand.

[7] Hogg, S., (2014). "Seismically resilient building technology: examples of resilient buildings constructed in New Zealand since 2013. In *Proceedings 10th Pacific Conference on Earthquake Engineering Building an Earthquake-Resilient Pacific*, Sydney, Australia.

[8] Wiebe, L., (2015). "Design and construction of controlled rocking steel braced frames in New Zealand". In *Proceeding of the Second ATC & SEI Conference on Improving the Seismic Performance of Existing Buildings and Other Structures*, San Francisco, CA, USA.

[9] SCNZ, *SCNZ-110:2015, Design Guide for Controlled Rocking Systems*, Steel Construction New Zealand, Manukau City, New Zealand, 2015.

[10] Roke, D. A. (2010). *Damage-free seismic-resistant self-centering concentrically-braced frames*. Lehigh University.

[11] Zhang, C., Steele, T.C., Wiebe, L.D.,(2018). "Design-level estimation of seismic displacements for self-centring SDOF systems on stiff soil". *Engineering Structures, 177*, 431-443.

[12] Steele, T.C., and Wiebe, L., (2016). "Dynamic and equivalent static procedures for capacity design of controlled rocking steel braced frames". *Journal of Earthquake Engineering and Structural Dynamics, 45*(15), 2349-2369.

[13] Mottier, P., Tremblay, R., and Rogers, C. (2018). "Seismic retrofit of low-rise steel buildings in Canada using rocking steel braced frames". *Earthquake Engineering & Structural Dynamics*, *47*(2), 333-355.

[14] Mottier, P., Tremblay, R., and Rogers, C. A. (2018). "Shake Table Test of a Half-Scale 2-Storey Steel Building Seismically Retrofitted Using Rocking Braced Frame System". In *Key Engineering Materials* (Vol. 763, pp. 466-474). Trans Tech Publications.

[15] American Society of Civil Engineers -ASCE (2016). *Minimum design loads for buildings and other structures*, *ASCE/SEI Standard 7–16*. Prepared by the American Society of Civil Engineers, Reston, VA, United States.

[16] AISC Committee. (2016). Specification for structural steel buildings (ANSI/AISC 360-16). *American Institute of Steel Construction, Chicago-Illinois*.

[17] OpenSees. (2015). Open system for earthquake engineering simulation v2.4.5 [computer software]. http://opensees.berkeley.edu/

[18] FEMA P695 (2009). *Quantification of building seismic performance factors*. Report No. FEMA P695, Federal Emergency Management Agency, Washington, D.C.

[19] Meier, J. H. (1945). "On the dynamics of elastic buckling". *J. Aeronaut. Sci., 12*, 433-440.